International Journal of Heat and Fluid Flow 30 (2009) 1099–1105

Contents lists available at ScienceDirect

International Journal of Heat and Fluid Flow

journal homepage: www.elsevier.com/locate/ijhff

An experimental study of large area source turbulent plumes

N.B. Kaye [a,*], G.R. Hunt [b]

[a] Department of Civil Engineering, Clemson University, Clemson, SC 29634, USA
[b] Department of Civil and Environmental Engineering, Imperial College London, London SW7 2AZ, UK

ARTICLE INFO

Article history:
Received 2 February 2009
Received in revised form 19 May 2009
Accepted 25 May 2009
Available online 2 July 2009

Keywords:
Turbulent plumes
Area source
Convection

ABSTRACT

A series of experiments was performed to measure the rate of entrainment of ambient fluid into a negatively buoyant turbulent plume emerging from a large area source with low initial momentum flux, a so called 'lazy plume'. Immediately below the source, the plume contracts until it reaches a neck of diameter approximately half the source diameter. Beyond the neck it expands, eventually forming a classic pure plume with linear radial growth rate. The variation of volume flow rate, Q, with vertical distance from the source, z, was measured in the near source region, between the source and the neck for different source values of Γ_0, equivalent to the source Richardson number. Experiments were run for $10^5 < \Gamma_0 < 5 \times 10^7$. Our results indicate that the volume flux in the plume increases linearly from the source to the neck, that is, $Q \propto z$. This scaling is in contrast to pure plumes where the flow rate increases as $Q \propto z^{5/3}$. Our experimental results collapsed onto a single line when scaled, giving an empirical expression for the near source flow rate of the form $Q \propto \Gamma_0^{1/3} z$. We discuss this result in relation to the classic entrainment model for turbulent plumes and show that modifications to existing closure schemes are required for lazy plumes.

1. Introduction

Turbulent plumes play a major role in convection problems, from the rise of hot ash clouds due to volcanic eruptions to hot air rising above a person sitting at a desk. Much work has been done to understand these flows in a wide variety of industrial, environmental, and geophysical settings. For example, work on air movement and ventilation flows in buildings (Linden et al., 1990), shows that plumes in a ventilated room create a stable thermal stratification that induces a ventilation flow. In their model the authors assume that the plumes are ideal point sources of heat and that the classical plume model of Morton et al. (1956) could be used to predict the volume flux and buoyancy of the plume. However, not all heat sources in a room can be considered point sources. For example, a patch of sunlight shining on the floor will produce a thermal plume, but not a point source plume. The ventilation flow established is sensitive to the distribution of the heat input and it is therefore important to understand how the volume flow rate and buoyancy vary with height above such area sources. In this paper we consider large area source plumes that are highly lazy, that is, plumes with a source radius much larger than their momentum jet length, defined by Baines and Turner (1969) as $L_m \propto M_0^{3/4} F_0^{-1/2}$ where M_0 is the source momentum flux and F_0 is the source buoyancy flux.

A classical approach to modelling Boussinesq turbulent plumes was presented by Morton et al. (1956) who developed integral equations for the fluxes of volume, momentum and buoyancy of an axisymmetric turbulent plume arising from a point source of buoyancy into still surroundings. The model of Morton et al. (1956) assumes that Reynolds stresses dominate viscous shear stresses and that the plume flow is fully developed with self-similar profiles of velocity, buoyancy and Reynolds stress at all heights. The system of equations was closed using the entrainment assumption that states that the mean horizontal velocity of ambient fluid being entrained into the plume u_e is proportional to the mean vertical velocity of the plume at that height w. That is, the rate of increase of volume flux with height is given by

$$\frac{\mathrm{d}\pi b^2 w}{\mathrm{d}z} = 2\pi b u_e \quad \text{where } u_e = aw \tag{1}$$

The entrainment coefficient α is typically assumed to be a constant. Although the model of Morton et al. (1956) was developed assuming a fully developed self-similar turbulent plume, the model has been applied to other flows that are not self-similar such as fountains (Bloomfield and Kerr, 2000), plumes in a stratified environment (Caulfield and Woods, 1998), and the near source adjustment region (Morton, 1959; Hunt and Kaye, 2001) of the plume.

Extensions to Morton et al. 1956 have been proposed in the form of variable entrainment coefficient models, see for example List and Imberger (1973) and Kaminski et al. (2005). These typically involve expressing the entrainment coefficient as a function of the local plume Richardson number

* Corresponding author.
E-mail address: nbkaye@clemson.edu (N.B. Kaye).

0142-727X/$ - see front matter © 2009 Elsevier Inc. All rights reserved.
doi:10.1016/j.ijheatfluidflow.2009.05.001

Nomenclature

b	plume radius (m)	Ri	Richardson number (–)
C_p	specific heat of air (J/kg K)	u_e	entrainment velocity (m/s)
F	plume buoyancy flux ($m^4\ s^{-3}$)	w	mean vertical velocity (m/s)
g	gravitational acceleration (m/s^2)	z	distance from plume source (m)
g'	fluid buoyancy (m/s^2)	α	entrainment coefficient (–)
L_m	momentum jet length (m)	Γ	flux balance parameter: Ri (–)
L_q	source length scale (m)	ξ	scaled vertical distance (–)
M	plume momentum flux ($m^4\ s^{-2}$)	ρ	plume fluid density (kg/m^3)
P	plume source heat output (W)	ρ_a	ambient fluid density (kg/m^3)
Q	plume volume flux (m^3/s)		
q	scaled plume volume flux (–)		

$$Ri = \frac{g'b}{w^2} \tag{2}$$

where b is the 'top hat' radius and g' is the buoyancy given by

$$g' = g\frac{\rho - \rho_a}{\rho_a} \tag{3}$$

Here ρ is the density of the plume fluid, ρ_a is the ambient fluid density, and g is the acceleration due to gravity. These models have focused on the transition from jet-like to plume-like behavior in flows of buoyant fluid with a relatively high initial momentum flux, so-called 'forced plumes'. Very little work has considered the entrainment of plumes with very low source momentum flux.

In this paper we consider the problem of highly lazy turbulent plumes, that is, plumes that originate from finite area sources with relatively low momentum flux. The degree of 'laziness' is characterized by the non-dimensional parameter

$$\Gamma_0 = \frac{5}{8\alpha}\frac{Q_0^2 F_0}{M_0^{5/2}} \tag{4}$$

where Q is the volume flux, F is the buoyancy flux and M is the momentum flux – the subscript '0' denoting the source value, i.e. at $z = 0$. For thermal plumes the buoyancy flux of the source can be calculated from the heat output following (Batchelor, 1954). The buoyancy flux $F_0 = Pg\beta/(C_p\rho_a)$ where P is the heat output (W), C_p is the specific heat of air at constant pressure, and β is the coefficient of thermal expansion for the fluid (in air $\beta = 1/T_a$ where T_a is the ambient temperature in Kelvin). For sources that yield $\Gamma_0 > 1$ the plume is considered lazy and for $\Gamma_0 < 1$ it is forced. See Morton and Middleton (1973) and Hunt and Kaye (2005) for a more detailed discussion of plume classification. The parameter Γ_0 is equivalent to the source Richardson number.

There have been a number of recent experimental studies of lazy area source plumes, see Colomer et al. (1999), Friedl et al. (1999), and Epstein and Burelbach (2001). Each of these papers has a different motivation ranging from large scale oceanic and atmospheric convection to mixing above accidental leaks from gas storage facilities. All three papers observe that the flow contracts as it moves away from the source reaching a minimum radius, or neck. Beyond the neck the plume begins to expand eventually forming a pure plume with the radius growing linearly with height. The consensus of Colomer et al. (1999), Friedl et al. (1999) and Epstein and Burelbach (2001) is that the neck height is approximately equal to one source radius and the neck has a radius of approximately half the source radius. Furthermore, these measurements were independent of Γ_0. Beyond these basic geometric results, Colomer et al. (1999), Friedl et al. (1999) and Epstein and Burelbach (2001) have few measurements in common. None of these papers presents measurements of the volume flux in the near source region which is key to understanding the rate of entrainment of ambient fluid into the plume.

Various theoretical models have been used to describe highly lazy plumes. For example, Epstein and Burelbach (2001) used a boundary layer approach to describe the contraction above the source. The most commonly used model applied to plumes with high values of Γ_0 is that of Morton et al. (1956). See for example, Hunt and Kaye (2005) and Fannelop and Webber (2003). The results of these models show good qualitative agreement with experimental results. They predict a necking of the plume a short distance from the source, albeit a function of Γ_0, and a far field flow that behaves like a pure plume. However, the models' quantitative predictions, including of the plume volume flux, have not been rigorously validated.

In this paper we present results of a series of experiments that directly measured the volume flux in lazy plumes for a broad range of Γ_0. In Section 2 we describe our experimental technique as well as the setup and procedure for running the experiments. The results of these experiments are presented in Section 3 together with a brief discussion of the scaling required to collapse the data. The results are discussed in Section 4 and conclusions drawn in Section 5.

2. Experimental setup and technique

A series of experiments was conducted to measure the volume flow rate in the near source region of highly lazy plumes using the technique developed by Baines (1983). The goal of these experiments was to establish the functional relationship between the plume flow rate at a given distance from the source and the source conditions. The experiments were conducted using salt water releases from area sources in fresh water environments in order to form the density difference and the release stained with a dye for flow visualization. Five sets of experiments were run for $\Gamma_0 = 9.1 \times 10^4$, 1.6×10^5, 5.4×10^5, 5.7×10^6 and 5.4×10^7.

The plume was formed by passing a salt water solution of known density through a nozzle into a large glass-sided visualization tank containing a still body of fresh water. The plume and tank fluids were at the same temperature. The plume salt water solution was dyed using a blue food coloring. The density of the source and ambient fluid was measured using an Anton Paar DMA 35 N density meter to an accuracy of 5×10^{-4} g cm^{-3}. The density of the salt solution was in the range 1.015–1.083 g cm^{-3}. The salt solution was supplied by a constant head gravity feed with a total head of approximately 2.5 m. The plume supply flow rate was controlled by a needle valve and measured using an in-line rotameter flow rate meter. Typical source flow rates were in the range 1.4–15.2 cm^3/s.

The plume nozzle was designed specifically to create a uniform velocity profile across the exit plane of the source. The nozzle body was constructed from a section of PVC pipe sealed at one end except for an inlet for the plume fluid. The nozzle outlet was a 152 mm diameter disc made of 5 mm thick sintered stainless steel

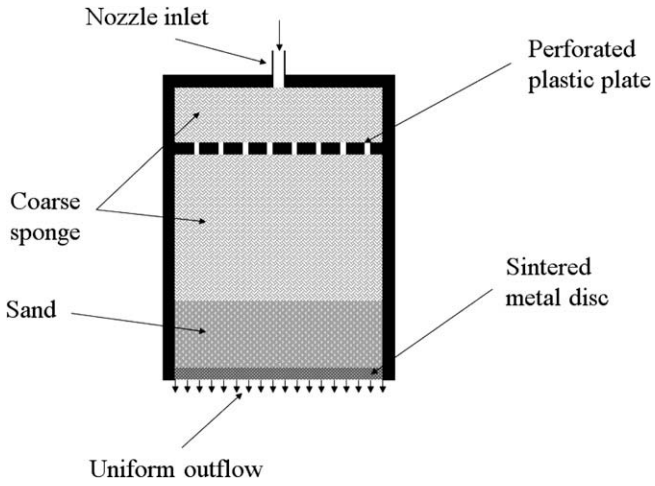

Fig. 1. Schematic diagram of the plume nozzle used to create a highly lazy plume with a uniform velocity profile at the source.

(40 μm powder size GKN sintered metals part number SIKA M40AX). Inside the nozzle was a series of coarse sponges to disperse the momentum from the nozzle inlet pipe followed by a layer of sand. This design ensured that the bulk of the pressure loss in the nozzle was in the sand layer and the sintered metal plate. The pressure loss was therefore evenly distributed across the area of the nozzle ensuring a uniform outlet velocity. A schematic of the nozzle design is shown in Fig. 1 and a series of images of the initial outflow showing the uniformity of flow is shown in Fig. 2.

The volume flow rate in the plume was measured using the method of Baines (1983). This technique involves activating a steady plume source in a visualization tank in which there is a net co-flow in the ambient fluid, i.e. in the same direction as the plume flow. A two-layer stratification forms in the tank that, after an initial transient period, settles with the density interface at a constant distance from the plume source. As the stratification is stable, the only way fluid can pass across the density interface is through the plume. Therefore the volume flow rate in the plume at the height of the interface is equal to the known volume flow rate of the co-flowing ambient. This is the forced ventilation analogue of the natural ventilation flow presented by Linden et al. (1990).

In our experiments, fresh water was added at the top of the visualization tank using a constant head tank and at a steady rate measured using an in-line flow-meter. Fluid was removed from the base of the tank at the same rate using a number of siphons operating in parallel. The rate at which fluid was removed was also measured using rotameter flow rate meters. The inlet and outlet flow rates were closely balanced throughout each experiment. Any minor imbalance resulted in small changes in the depth of the tank, though they did not affect the measured flow rates (taken to be the flow rate of the fluid extracted from the base of the tank). Care was also taken to ensure that the fresh ambient fluid added at the top of the tank had negligible vertical momentum. This ensured that the inlet ambient co-flow did not create mixing at the density interface or create background turbulence through which the plume would descend. The momentum was minimized by feeding the fluid into the tank through a porous hose, with the hose outlet flowing over a flat plate with a series of holes in it. Despite these precautions we were still only able to maintain a stable interface for a co-flow rate of up to approximately 150 cm^3/s, though this value varied from experiment to experiment. For the lower values of Γ_0 considered we had to use lower source buoyancy flux values, and therefore the density jump across the interface was lower. In these cases we were limited to co-flow rates of less than 150 cm^3/s. A schematic of our experimental setup is shown in Fig. 3.

The same procedure was adopted for running each experiment. An experiment was started by turning on the plume salt supply and setting the desired volume flow rate using the needle valve attached to the flow rate meter. A plume was observed to form below the nozzle and a filling box flow developed (cf. Baines and Turner, 1969) with a dense salty layer forming at the bottom of the visualization tank. This layer was allowed to deepen, and the interface to approach the nozzle. Once the interface was close to the nozzle – typically 1–5 cm below – the ambient co-flow was turned on. A timer was started and the system was left to adjust for approximately 20 min. During this time regular checks were made on all the flow rate meters to ensure they were stable. After this settling time the distance from the interface to the nozzle was measured by eye, to within half a millimeter, using a ruler taped to the side of the tank. This measurement was repeated every 5 min until the measurement stopped changing from one recording to the next. The flow was now assumed to have reached a steady state, and this distance was taken to be the final measurement. The outflux from the base of the tank was measured using a stop-watch and measuring cylinder, to verify that the flow rate measured using the rotameters was correct. This additional flow rate measurement was to check if there was any flow rate reading variation due to the small

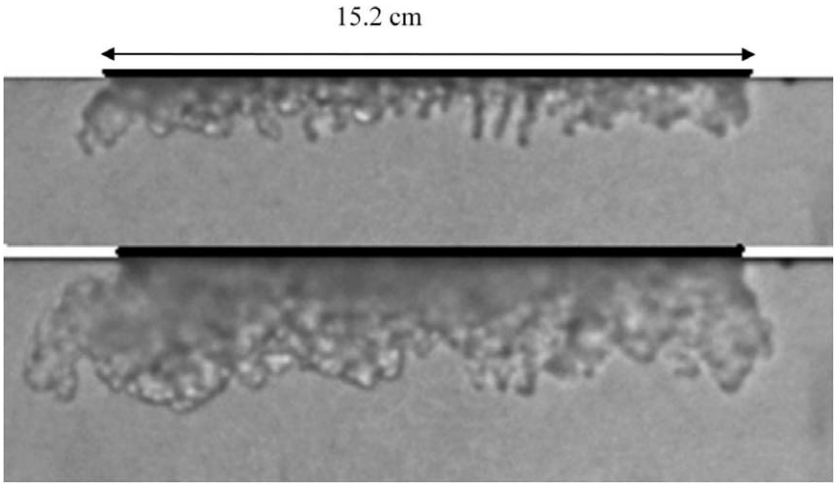

Fig. 2. A pair of images showing the initial uniform outflow of dense salt water from the nozzle.

change in density in the outflow due to the plume fluid. The flow rate measured using the stop-watch and measuring cylinder was taken to be the ambient flow rate.

Once the initial measurement was completed the co-flow rate was increased by 1 l/min and the settling and measurement procedures were repeated. After each measurement the co-flow flow rate was increased until we were no longer able to maintain a stable density interface. At this point the co-flow rate was reduced by ½ l/min and then by 1 l/min increments until the co-flow rate was ½ l/min. The flow rate was then increased by ½ l/min and then by 1 l/min increments until the initial flow rate was reached. This meant that we had flow rate measurements in ½ l/min increments. This procedure also provided a check on our settling time as half the measurements were made with the interface rising between measurements (due to reductions in the co-flow volume flux) and half with the interface falling (due to the increases in the co-flow volume flux). If the interface had not stabilized when we took each measurement the results would have shown some hysteresis. As such a variation was not systematically evident in our measurements we are confident that the flow had fully settled when each measurement was made.

The source conditions were then adjusted and the entire procedure repeated.

All distance measurements were made directly by eye using a ruler taped to the tank. However, a couple of visualization experiments were run to verify the uniformity of the outflow. The experimental setup was identical except that there was no co-flow. The plume was turned on and filmed until the ambient started to fill up with plume fluid, a period of about 20 s. The images were then processed to account for background variations in lighting and the light attenuation was calculated using the DigiFlow system (Dalziel, 1993). See Hacker et al. (1996) for more details on the light attenuation technique for measuring buoyancy. The resulting video was time averaged to produce an image of the mean buoyancy profile of the plume. As the images were only used as a check on the uniformity of the outflow and to verify that the plume was axisymmetric, detailed calibration and re-scaling were not performed. A typical image of the mean buoyancy is shown in Fig. 4. The image clearly shows the contraction above the source and an axisymmetric plume. Measuring the exact location and radius of the neck requires fitting Gaussian curves to the buoyancy profile at each height and then calculating the standard deviation of the curve. We did not do these calculations as there are already a number of neck height measurements in the literature that show good agreement (Colomer et al., 1999; Friedl et al., 1999; Epstein and Burelbach, 2001).

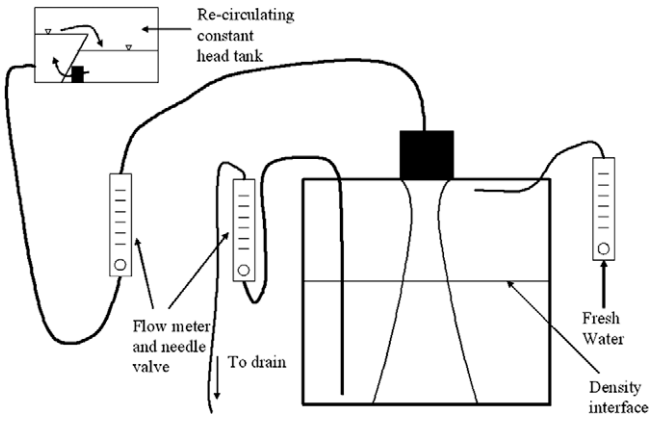

Fig. 3. Experimental setup used for measuring the volume flux of the plume at various distances from the source using the method of Baines (1983). The visualization tank is 1.8 m deep and has a square base of side length 1.25 m.

3. Experimental results

The flow observed in our experiments is similar to that observed by Colomer et al. (1999) and Friedl et al. (1999). The fluid came out of the nozzle with a uniform velocity as a slug flow (cf. Fig. 2). The fluid fell away from the nozzle and mixed in a manner visually similar to Rayleigh–Taylor flow. The flow grew laterally and formed a thermal-like structure at the end of the plume. Behind this cap a plume flow developed. The flow began to contract and a neck formed. The neck moved toward the nozzle over time and settled at a distance of approximately one source radius from the nozzle. The neck location and radius did not appear to vary between experiments despite changing Γ_0 by almost three orders of magnitude. All these observations are identical to those described by Colomer et al. (1999) for the initial flow development. As a consequence we did not make any detailed measurements during this phase of the flow, or of the neck location as these parameters are well documented in the literature.

A series of five experiments were run in which multiple volume flow rate measurements were made. Each experiment was run for a different value of Γ_0. To vary Γ_0 both the buoyancy of the source fluid (g'_0) and the source volume flux (Q_0) were varied. In order to present the results in a consistent manner, the measured volume flow rates were scaled on the plume source volume flow rate to yield the dimensionless volume flux $q = Q/Q_0$. For a pure point source plume in an unstratified ambient there is no vertical length scale associated with the source on which to scale vertical distance. However, for a source of finite horizontal extent there are two pertinant length scales, the momentum jet length $L_m = M_0^{3/4}/F_0^{1/2}$ (see Morton, 1959) and the source flow rate length, namely

$$L_q = \frac{5b_0}{6\alpha} = \frac{Q_0}{M_0^{1/2}} \tag{5}$$

which represents the distance from the actual physical source to the virtual origin of a pure plume ($\Gamma_0 = 1$) of source radius b_0. The parameter Γ_0 is the ratio of the square of these two length scales ($\Gamma_0 \sim L_q^2/L_m^2$). For highly lazy plumes (large Γ_0) $L_q \gg L_m$. Therefore, vertical distances from the source (z) are scaled on L_q. The scaled height is thus

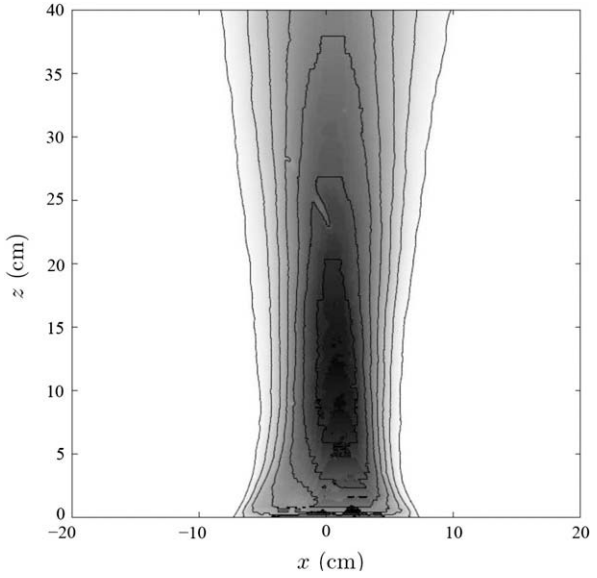

Fig. 4. An inverted, unscaled contour plot of a plume, with $\Gamma_0 = 1.6 \times 10^5$, showing mean buoyancy (shading) and contours of constant mean buoyancy (lines).

$$\xi = \frac{z}{L_q} \tag{6}$$

See Hunt and Kaye (2001, 2005) for more details on virtual origins and the appropriateness of this length for scaling vertical distances from the source. Although the entrainment coefficient (α) is known to vary with (Γ_0) we can, without loss of generality, use the pure plume ($\Gamma_0 = 1$) value for α when calculating the source parameter Γ_0, and the length scale L_q as, for any given experiment, these two parameters are constant.

The data measured for each of the five experiments is shown in Fig. 5. There is clearly significant variation in the rate of entrainment into the plume with Γ_0. It is also clear that the flow rate increases approximately linearly with height for any given Γ_0. We would therefore expect the flow rate data to collapse when plotted against a linear function of ξ and an unknown function of Γ_0, that is, $q = \xi f(\Gamma_0)$.

The flow rate at any given height will be a function of the vertical distance from the source and the source fluxes, i.e.

$$Q = Q(z, Q_0, M_0, F_0) \tag{7}$$

where the source radius can be written in terms of the source volume and momentum fluxes ($b_0 = Q_0/\sqrt{M_0}$). As the nozzle used in the experiments had a fixed radius, it was not possible to vary the volume flux and momentum flux independently. It was, however, possible to vary the buoyancy flux independently of the volume and momentum fluxes.

Dimensional analysis allows us to re-write this expression in terms of non-dimensional groups

$$\frac{Q}{F_0^{1/3} L_q^{5/3}} = f\left(\frac{z}{L_q}\right) \quad \text{or} \quad \frac{q}{\Gamma_0^{1/3}} = f(\xi) \tag{8}$$

Despite the fixed nozzle radius, we were able to vary the controlling non-dimensional parameters (Γ_0 and ξ) independently of each other.

Although dimensional analysis tells us nothing of the form of the function $f(z/L_q)$, we have established that, in general, $q \propto \Gamma_0^{1/3}$ at any height. We would, therefore, expect that plotting q against $\Gamma_0^{1/3}\xi$ would collapse our data onto a single curve. This is indeed the case as shown in the re-scaled data of Fig. 6.

The data shows a clear linear relationship and so a line was fitted through the re-scaled data, forced through $q = 1$ at $\xi = 0$ giving a fit of

$$q = 1 + 3.4\Gamma_0^{1/3}\xi \tag{9}$$

This is in stark contrast to the far field pure plume relation $q \sim \Gamma_0^{1/3}\xi^{5/3}$ (from Morton et al., 1956). This suggests that as Γ_0 increases the local rate of entrainment decreases.

Our experimental result that the volume flow rate in the plume increases linearly with distance from the source in the near source region disagrees with the constant entrainment coefficient result of Hunt and Kaye (2005), which predicted negligible entrainment for large Γ_0 and, therefore, an essentially constant flow rate in the very near source region. Our experimental results (9) also imply that the mean buoyancy should vary inversely proportional to the distance from the source ($g' \propto z^{-1}$) as the buoyancy flux is constant with height and therefore $Qg' = const$.

4. Discussion

We now discuss our experimental results in relation to existing theoretical work on turbulent plumes. We begin by comparing our results with existing theoretical predictions. We show that both constant α and existing variable α models do not adequately describe the plume in the near source region of lazy plumes. We then discuss the implications of our results for calculations of the virtual origin for highly lazy plumes.

4.1. Entrainment coefficient

It was shown by Hunt and Kaye (2005) that the model of Morton et al. (1956) applied to highly lazy plumes gives a solution with negligible entrainment in the near source region. This is in stark contrast to the experimental results presented in this paper suggesting that the constant entrainment coefficient formulation of the plume conservation equations of Morton et al. (1956) are inappropriate for large Γ_0. This is also true of existing variable entrainment coefficient models. For example, List and Imberger, (1973) and Kaminski et al. (2005) suggest that locally $\alpha = \alpha(Ri) = \alpha(\Gamma)$ and that the function $\alpha(\Gamma)$ is linear and increases with increasing Γ. The closures (List and Imberger 1973; Kaminski et al., 2005) were developed to model the transition of a highly forced buoyant jet flow into a pure plume flow. That is, they were designed for source conditions with $0 < \Gamma_0 < 1$. This $\alpha(Ri)$ variable entrainment coefficient model has been used to account for the experimentally measured differences in α between jets and plumes. However, for highly lazy plumes, Γ_0 can be very large ($\Gamma_0 > 10^7$ at the source in our experiments).

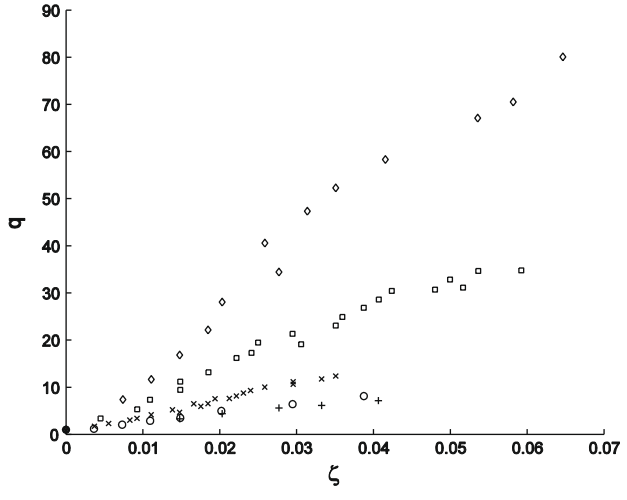

Fig. 5. Plume flow rate scaled on the source flow rate as a function of scaled height. The symbols indicate the different values of Γ_0 and are given by (◇) $\Gamma_0 = 5.4 \times 10^7$, (□) $\Gamma_0 = 5.7 \times 10^6$, (×) $\Gamma_0 = 5.4 \times 10^5$, (○) $\Gamma_0 = 1.6 \times 10^5$, and (+) $\Gamma_0 = 9.1 \times 10^4$.

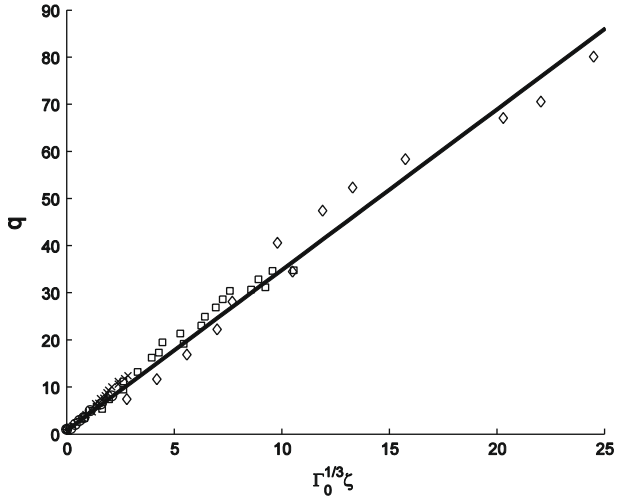

Fig. 6. Scaled plume flow rate plotted against $\Gamma_0^{1/3}\xi$. The symbols are the same as for Fig. 5. The line is $q = 1 + 3.4\ \Gamma_0^{1/3}\xi$.

The models of List and Imberger (1973) and Kaminski et al. (2005) would therefore lead to values of $\alpha \propto O(10^6)$ which is clearly unrealistically high and unbounded in the limit of a zero momentum flux source such as a heated plate.

The inapplicability of Morton et al. (1956) to highly lazy plumes is to be expected. The equations were developed for idealised long thin self-similar plumes, while highly lazy plumes are neither thin nor self-similar in the near source region. The entrainment process is also unlikely to be horizontal as the perimeter of the plume is bent in toward the source (see Fig. 4). Although a full theoretical model is beyond the scope of this paper, we believe that the key process will be a vertical mixing process similar to Rayleigh–Taylor mixing.

4.2. Virtual origin

We now turn to the problem of finding the virtual origin of a highly lazy plume. The virtual origin of a plume is the point from which the far field plume appears to originate. This problem has been addressed theoretically (Morton, 1959; Caulfield and Woods, 1995; Hunt and Kaye, 2001) using the plume conservation equations of Morton et al. (1956). For example, Hunt and Kaye (2001) developed series solutions for the plume volume flux at large distances from the source and then projected the flow rate back to locate the virtual origin. Their theoretical prediction compared well with a series of experiments, though the experiments were only run for $\Gamma_0 \leqslant 4$. The experimental results in this paper suggest that for large values of Γ_0 this model should not apply, and that the virtual origin, along with other geometric distances such as the neck height, should become independent of Γ_0.

The main problem with applying Morton et al. (1956) is that the flow is contracting above the source and the entrained inflow is not horizontal. However, it may be reasonable to assume that Morton et al. (1956) can be applied in regions where the flow is not contracting, that is, above the plume neck. It was shown by Caulfield (1991) that at the neck, $\Gamma = \Gamma_{neck} = 5/2$. Also, the experimental results of Hunt and Kaye (2001) showed good agreement with theory for $\Gamma_0 \leqslant 4$. This suggests that Morton et al. (1956) can reasonably be applied to plumes near and slightly below the neck. Until now we have only used Γ as a source condition. However, it is possible to calculate the volume, momentum and buoyancy fluxes at any height, and therefore, to calculate $\Gamma(\xi)$. We can therefore calculate the virtual origin of any lazy plume using Hunt and Kaye (2001) by calculating the virtual origin of the plume as if its source was the plume neck. Using previous measurements of neck height and radius (Colomer et al., 1999; Friedl et al., 1999; Epstein and Burelbach, 2001) we find that the virtual origin for all highly lazy plumes is at a distance

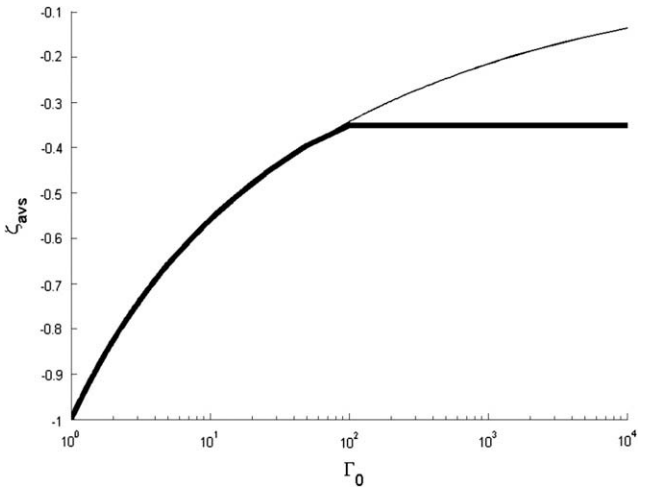

Fig. 7. Plume virtual origin location ξ_{avs} as a function of Γ_0. The thin line is the theoretical prediction of Hunt and Kaye (2001). The overlayed thick line is the empirical correction based on the neck height (10).

$$\xi_{\text{avs}} = -0.31 \tag{10}$$

below the source. This result is plotted in Fig. 7 along with the theoretical prediction of Hunt and Kaye (2001). Scaled directly on the source radius (b_0) Eq. (10) becomes $z_{\text{avs}} = -2.2b_0$. This result is almost identical to the experimental result of Bouzinaoui et al. (2007) who measured the far field radial growth rate of a thermal plume that formed above a heated disc ($\Gamma_0 = \infty$), projected these measurements back to a virtual origin and found that $z_{\text{avs}} = -2b_0$.

Clearly Eq. (10) does not intersect the theoretical prediction of Hunt and Kaye (2001) at $\Gamma_0 = 5/2$. This is because the neck height and radius only become constant fractions of the source radius for sufficiently large values of Γ_0. For intermediate values of Γ_0 the neck will be thicker and closer to the source and our correction will not apply. There will, therefore, be some transition away from the theoretical line toward the dashed line. The exact nature of this transition is beyond the scope of this paper. The far field volume flux will therefore be given by $q = \Gamma_0^{1/3}(\xi + \xi_{avs})^{5/3}$ following Morton et al. (1956), Hunt and Kaye (2001, 2005). We can therefore write an approximate expression to describe the volume flux at all heights

$$q\Gamma_0^{-1/3} = \begin{array}{ll} \Gamma_0^{-1/3} + 3.4\xi & \text{for} \quad \xi < 0.055 \\ (\xi + 0.31)^{5/3} & \text{for} \quad \xi > 0.055 \end{array} \tag{11}$$

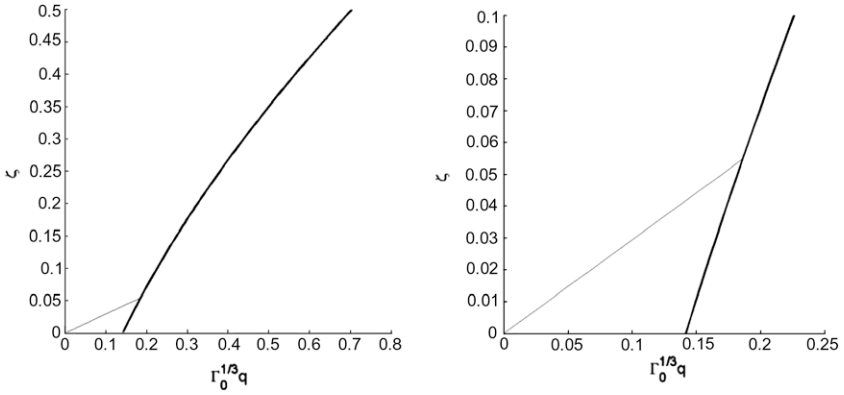

Fig. 8. Plots of $q\Gamma_0^{-1/3}$ vs ξ in the limit of $\Gamma_0 \to \infty$. The thick line is the pure plume volume flow rate solution $q \sim \Gamma_0^{1/3}\xi^{5/3}$ of Morton et al. (1956) with a virtual origin offset. The thin line is the near source volume flow rate in the limit of $\Gamma_0 \to \infty$ based on the experimental data presented in this paper: (a) the transition from the $q \sim \xi$ flow regime to the $q \sim \xi^{5/3}$ regime and (b) exploded view of plot (a) showing the transition between flow regimes at $\xi \approx 0.055$.

where the transition value of $\xi = 0.055$ is the height at which, in the limit of $\Gamma_0 \to \infty$, the two volume flux expressions match. Plots of Eq. (11) are shown in Fig. 8.

5. Conclusions

We have presented experimental measurements of the near source volume flow rate for large area highly lazy plumes. Near the source the flow contracts to a neck and then begins to expand with increasing distance from the source. Our qualitative measurements of the flow perimeter indicate that the neck height and radius are independent of the source Richardson number (Γ_0), which is in agreement with existing published data (Colomer et al., 1999; Friedl et al., 1999; Epstein and Burelbach, 2001). Our measurements of the volume flow rate in the near source region are the first comprehensive set available. Our results indicate that near the source, the flow rate increases linearly with height and with the cube root of the source Richardson number. That is $Q \propto \Gamma_0^{1/3} z$, see Eq. (9).

Based on these measurements we proposed an empirical expression for the virtual origin of a highly lazy plume. The expression assumes that the model of Morton et al. (1956) can be applied downstream of the plume neck and uses the result of Hunt and Kaye (2001). This leads to $\xi_{avs} = -0.31$ for $\Gamma_0 \gg 1$. This is in excellent agreement with experimental results published for highly lazy thermal plumes (see Bouzinaoui et al., 2007) giving us confidence in this result.

The primary goal of this paper is to present experimental measurements of plume flow rate as a function of distance from the source, source buoyancy flux, and source Richardson number (Γ_0). Based on our results, we have shown that the classic plume conservation equations of Morton et al. (1956) are not valid in the near field for highly lazy plumes. Existing second order closures (List and Imberger, 1973; Kaminski et al., 2005) are also physically unrealistic. Further theoretical modeling work is required.

Acknowledgement

G.R.H. and N.B.K. would like to thank the EPSRC and the Nuffield foundation (Grant No. NAL/00586/G) for their support of this research.

References

Baines, W.D., 1983. A technique for the direct measurement of volume flux of a plume. J. Fluid Mech. 132, 247–256.
Baines, W.D., Turner, J.S., 1969. Turbulent buoyant convection from a source in a confined region. J. Fluid Mech. 37, 51–80.
Batchelor, G.K., 1954. Heat convection and buoyancy effects in fluids. Quart. J. Roy. Meteor. Soc. 80, 339–358.
Bloomfield, L.J., Kerr, R.C., 2000. A theoretical model of a turbulent fountain. J. Fluid Mech. 424, 197–216.
Bouzinaoui, A., Devienne, R., Fontaine, J.R., 2007. An experimental study of the thermal plume developed above a finite cylindrical heat source to validate the point source model. Exp. Therm. Fluid Sci. 31, 649–659.
Caulfield, C.P., Woods, A.W., 1995. Plumes with non-monotonic mixing behaviour. Geophys. Astrophys. Fluid Dyn. 79, 173–199.
Caulfield, C.P., Woods, A.W., 1998. Turbulent gravitational convection from a point source in a non-uniformly stratified environment. J. Fluid Mech. 360, 229–248.
Colomer, J., Boubnov, B.M., Fernando, H.J.S., 1999. Turbulent convection from isolated sources. Dyn. Atmos. Oceans 30, 125–148.
Caulfield, C.P., 1991. Stratification and Buoyancy in Geophysical Flows. Ph.D. Thesis, University of Cambridge, UK.
Dalziel, S.B., 1993. Rayleigh-Taylor instability: experiments with image analysis. Dyn. Atmos. Oceans 20, 127–153.
Epstein, M., Burelbach, J.P., 2001. Vertical mixing above a steady circular source of buoyancy. Int. J. Heat Mass Transf. 44 (3), 525–536.
Fannelop, T.K., Webber, D.M., 2003. On buoyant plumes rising from area sources in a calm environment. J. Fluid Mech. 497, 319–334.
Friedl, M.J., Hartel, C., Fannelop, T.K., 1999. An experimental study of starting plumes over area sources. Nuovo Cimento C 22, 835–845.
Hacker, J., Linden, P.F., Dalziel, S.B., 1996. Mixing in lock-release gravity currents. Dyn. Atmos. Oceans 24, 183–195.
Hunt, G.R., Kaye, N.G., 2001. Virtual origin correction for lazy turbulent plumes. J. Fluid Mech. 435, 377–396.
Hunt, G.R., Kaye, N.B., 2005. Lazy Plumes. J. Fluid Mech. 533, 329–338.
Kaminski, E., Tait, S., Carazzo, G., 2005. Turbulent entrainment in jets with arbitrary buoyancy. J. Fluid Mech. 526, 361–376.
Linden, P.F., Lane-Serff, G.F., Smeed, D.A., 1990. Emptying filling boxes, the fluid mechanics of natural ventilation. J. Fluid Mech. 212, 309–335.
List, E.J., Imberger, J., 1973. Turbulent entrainment in buoyant jets and plumes. J. Hydraul. Div. Proc. ASCE 99, 1461–1474.
Morton, B.R., 1959. Forced plumes. J. Fluid Mech. 5, 151–163.
Morton, B.R., Middleton, J., 1973. Scale diagrams for forced plumes. J. Fluid Mech. 58, 165–176.
Morton, B.R., Taylor, G.I., Turner, J.S., 1956. Turbulent gravitational convection from maintained and instantaneous sources. Proceedings of the Royal Society of London. Series A 234, 1–23.